Separation Science and Technology
Publication details, including instructions for authors and subscription information:
http://www.informaworld.com/smpp/title~content=t713708471

Optimization of Injection Conditions in Preparative Liquid Chromatography

G. Cretier[a]; J. L. Rocca[a]
[a] Laboratoire des Sciences Analytiques Université Claude Bernard Lyon I, Villeurbanne Cedex, France

To cite this Article Cretier, G. and Rocca, J. L.(1987) 'Optimization of Injection Conditions in Preparative Liquid Chromatography', Separation Science and Technology, 22: 8, 1881 — 1907
To link to this Article: DOI: 10.1080/01496398708057618
URL: http://dx.doi.org/10.1080/01496398708057618

SEPARATION SCIENCE AND TECHNOLOGY, 22(8-10), pp. 1881-1907, 1987

Optimization of Injection Conditions in Preparative Liquid Chromatography

G. CRETIER and J. L. ROCCA

LABORATOIRE DES SCIENCES ANALYTIQUES
UNIVERSITÉ CLAUDE BERNARD
LYON I, 69622 VILLEURBANNE CEDEX, FRANCE

Abstract

This paper describes the effect of injection volume on injectable sample load consistent with purity and recovery ratio of the solute of interest for different shapes of solute isotherms (convex or concave, without or with interactions between two adjacent solute bands). In preparative liquid chromatography, the column mass overloading conditions are usually thought to be better than volume overload conditions; according to this study, this statement is shown not to be true in all cases because optimization of injection conditions is much more complicated. For some isotherm shapes, there is an optimal injection volume in which injectable sample load is maximum.

INTRODUCTION

In preparative liquid chromatography, peak width is strongly influenced by the size of the injected sample. The latter can be increased in two ways: (a) by using a small injection volume and increasing the injected sample concentration, i.e., by mass overloading the column; or (b) by maintaining a concentration that lies in the linear part of the distribution isotherm and increasing the sample volume, i.e., by volume overloading the column. Gareil (*1*) and Cretier (*2*) have shown that mass overload conditions lead to higher amounts recovered per injection compared to those obtained under volume overload conditions if both isotherms are convex, i.e., the isotherm of the solute of interest (to be purified) and the isotherm of the impurity adjacently eluted (to be eliminated).

This paper deals with a more general discussion about the variations of the injectable sample load versus the injection volume for various isotherm shapes (convex, concave, and S-shaped). Moreover, the possible interactions between adjacent solute bands (mixed isotherm behavior) are considered. For each isotherm type, the optimal injection conditions are determined and the possible complications occurring from low solubility of the sample in the mobile phase are discussed.

THEORETICAL

Injectable Sample Load

In order to maintain the preparative specifications of the solute of interest, i.e., a given purity level p_0 and a given recovery ratio r_0, peak overlapping subsequent to column overload must be controlled. Thus a limiting charge Q_i (called the injectable sample load) and an optimal fractionation volume V_c (Fig. 1) can be defined from p_0 and r_0 requirements by Eqs. (1) and (2) when the first eluted solute (Solute A) is the solute of interest:

$$r_0 = \frac{Q_i - \int_{V_c}^{+\infty} c_A dV}{Q_i} \tag{1}$$

$$p_0 = \frac{rQ_i}{rQ_i + \int_0^{V_c} c_B dV} \tag{2}$$

or by Eqs. (3) and (4) when the second eluted solute (Solute B) is to be recovered:

$$r_0 = \frac{Q_i - \int_0^{V_c} c_B dV}{Q_i} \tag{3}$$

$$p_0 = \frac{rQ_i}{rQ_i + \int_{V_c}^{+\infty} c_A dV} \tag{4}$$

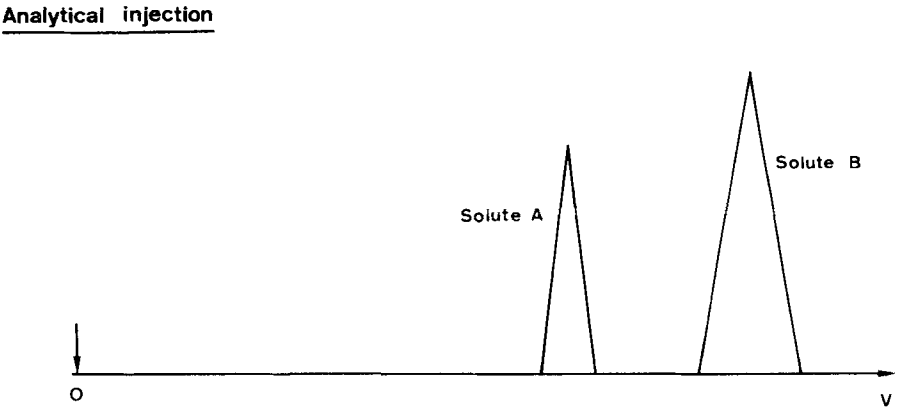

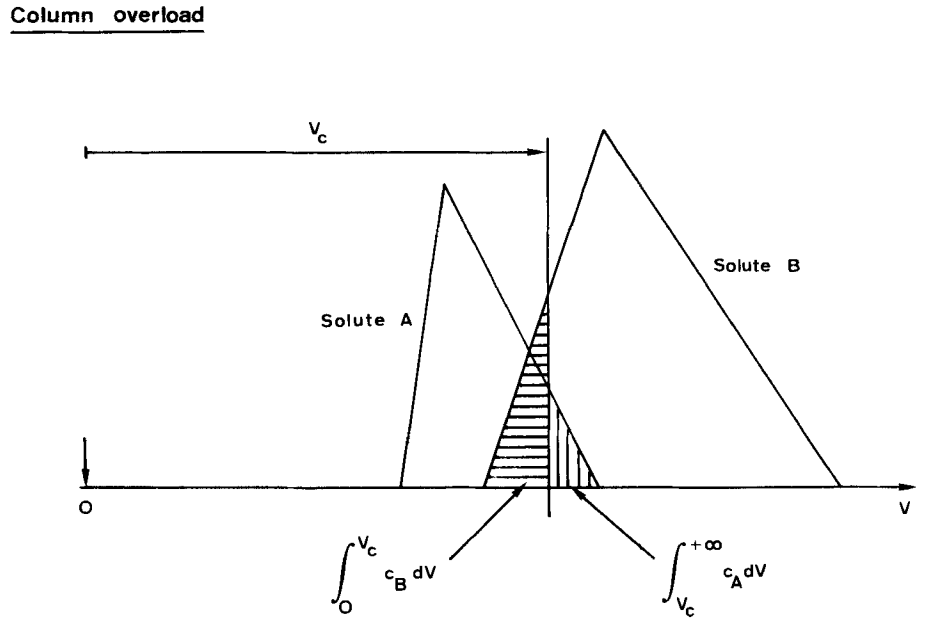

FIG. 1. Principle of column overload in preparative liquid chromatography.

c_A and c_B are the peak equation of Solutes A and B under column overload conditions, respectively, and V is the elution volume.

The calculation of the injectable sample amount Q_i and the optimal cut elution volume V_c requires the concentration profiles c_A and c_B to be known. From the Haarhoff-Van der Linde model it has been demonstrated that the reduced injectable load q_i (= Q_i/V_M, V_M being the column dead volume) depends only on the reduced injection volume v_i (= V_i/V_M, V_i being the actual injected volume), the theoretical plate number of the column N, and the nonlinearity of the solute distribution isotherms (*2*).

Solute Isotherm

The distribution isotherm of Solute j (j = A or B) is the plot of the concentration of j in the stationary phase, $C_{S,j}$, versus the concentration of j in the mobile phase, $c_{M,j}$, at the steady state for a given temperature. Figure 2 shows some isotherm shapes for a Solute j (*3*, *4*). Type L_j (Langmuir) isotherms are very usual in liquid chromatography, mainly when monolayer formation is favored over multilayer formation. The adsorption process is decreased with increasing solute concentration in the mobile phase (convex shaped) and stops after completion of the monolayer. Type $\bar{L}_j$ (anti-Langmuir) isotherms are less usual and are supposed to describe the solute distribution when the attractions between adsorbed solute molecules are stronger than solute-sorbent interactions. Consequently, solute adsorption increases with increasing adsorbate concentration (concave shaped). Type S_j (S-shaped) isotherms may be compared to type $\bar{L}_j$, but in this case the saturation of the stationary phase takes place for a relatively low concentration $C^0_{S,j}$ of the solute in the stationary phase. Each of these isotherms can be effectively represented by

$$C_{S,j} = \frac{a_j C_{M,j}}{1 + b_j C_{M,j}} \tag{5}$$

where the nonlinearity coefficient b_j is positive for type L_j and negative for types $\bar{L}_j$ and S_j. As experimentally found in most instances, isotherm approaches linearity for $C_{M,j} \to 0$. The term a_j is related to the capacity factor k'_j of the solute j according to

$$k'_j = \frac{1 - \varepsilon}{\varepsilon} a_j \tag{6}$$

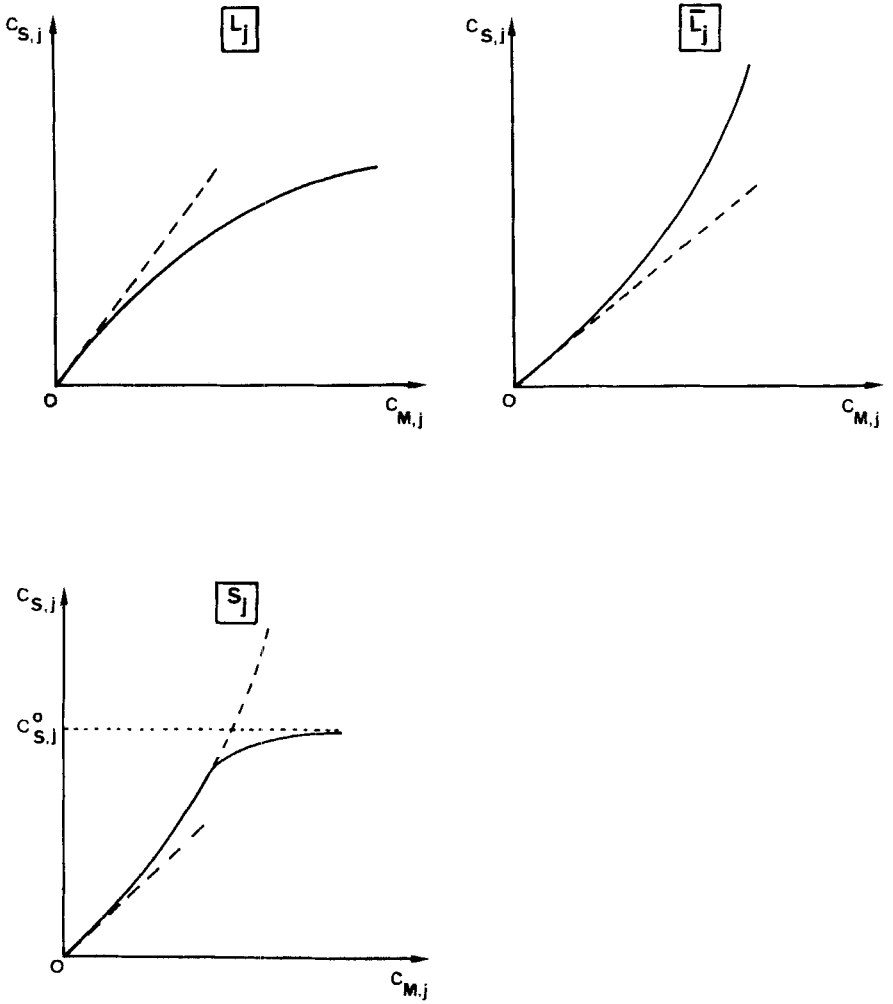

FIG. 2. Different isotherm shapes.

where ε is the total porosity of the chromatographic bed. The preceding isotherm equation (Eq. 5) assumes that the co-elution of two solutes occurs independently under overload conditions. When the two solutes migrate together at high concentration through a significant part of the column and compete for sites on the stationary phase, the distribution of Solute j between the phases may be affected by the concentration in the mobile phase of Solute k adjacently eluted (*5-10*) according to the mixed isotherm equation:

$$C_{S,j} = \frac{a_j C_{M,j}}{1 + b_j C_{M,j}\left(1 + c_{k/j}\frac{C_{M,k}}{C_{M,j}}\right)} \tag{7}$$

where $c_{k/j}$ is the interaction coefficient of k on j (j = A and k = B or j = B and k = A). Figure 3 shows the mixed isotherm of Solute j (noted M_j) for different $C_{M,k}/C_{M,j}$ values for $b_j > 0$ and $C_{k/j} > 0$ (which corresponds to very common conditions in liquid chromatography). When the ratio of the adjacently eluted solutes in the mobile phase $C_{M,k}/C_{M,j}$ decreases, the isotherm curvature decreases and the mixed isotherm M_j approaches the corresponding type L_j isotherm.

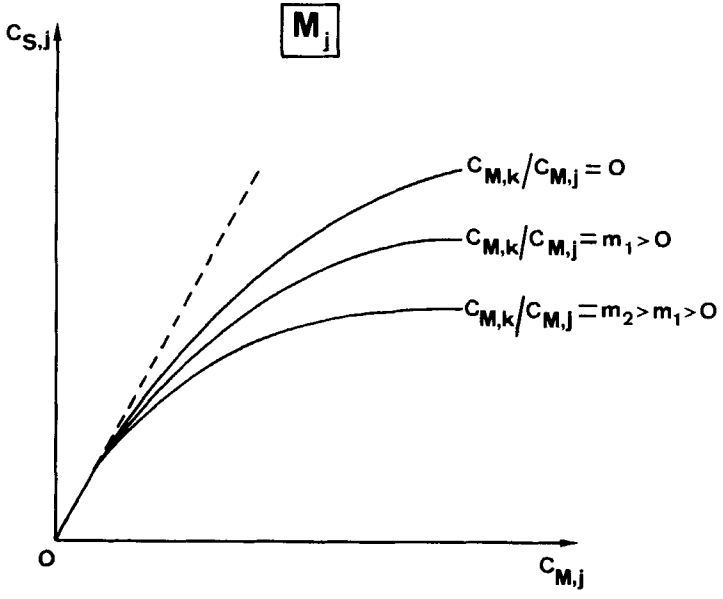

FIG. 3. Mixed isotherm of Solute j.

EXPERIMENTAL

Numerical Simulation of the Chromatographic Peak

The chromatographic simulation algorithm is based on a Craig-type repetitive distribution (*11*, *12*) summarized in Fig. 4. The column is divided into N_0 stages, each stage containing a volume ΔV_M of mobile phase ($\Delta V_M = V_M/N_0$) and a volume ΔV_S of stationary phase ($\Delta V_S = (1 - \varepsilon)\Delta V_M/\varepsilon$). The mobile phase approaching the column inlet is considered to be made up of a series of elemental elution volumes, each of them equal to the stage volume ΔV_M. The sample is assumed to have a rectangular concentration–volume profile in the mobile phase approaching the column (Fig. 4a) and is considered to be made up of a series of N_i elemental stage volumes ΔV_M ($N_i = V_i/\Delta V_M$), each of them containing the mass ΔQ_i ($\Delta Q_i = Q_i/N_i$, where Q_i is the amount injected). The chromatogram is developed by shifting the mobile phase against the stationary phase: the sample enters the column (Fig. 4b) and is distributed between phases according to its distribution isotherm (Fig. 4c). The process is continued (Figs. 4d and 4e) until a sufficient number of mobile phase transfers is performed to allow the sample to elute from the column. The simulated chromatogram is obtained by plotting the solute concentration in the mobile phase of the N_0th column stage versus the eluted volume V.

At any time during the development of a chromatogram, i.e., at any mobile phase transfer t, the following relationship can be written for any stage n of the column:

$$\varepsilon C_{M,j} + (1 - \varepsilon)C_{S,j} = \varepsilon C'_{M,j} \tag{8}$$

where $C'_{M,j}$ is the concentration of Solute j in the mobile phase of the $(n - 1)$th stage at the $(t - 1)$th transfer. For a sample containing two components A and B, Eqs. (5) and (8) (if A and B co-elute independently, Case 1) or (7) and (8) (if A and B interact during elution, Case 2), written for j = A and j = B as well, are solved simultaneously for each column stage at each mobile phase transfer to get the concentration of Components A and B in mobile and stationary phases. For Case 1, the system of four equations with four unknowns ($C_{M,A}$, $C_{S,A}$, $C_{M,B}$, and $C_{S,B}$) is reduced to two independent quadratic equations, one of the two roots of which has no physical meaning. In Case 2, the system of four nonlinear equations is solved by Powell's method (*13*).

Simulations were performed on a Harris 1000 computer (Harris Corp., Ft. Lauderdale, Florida, USA). The simulated column was a 15 cm × 4.6

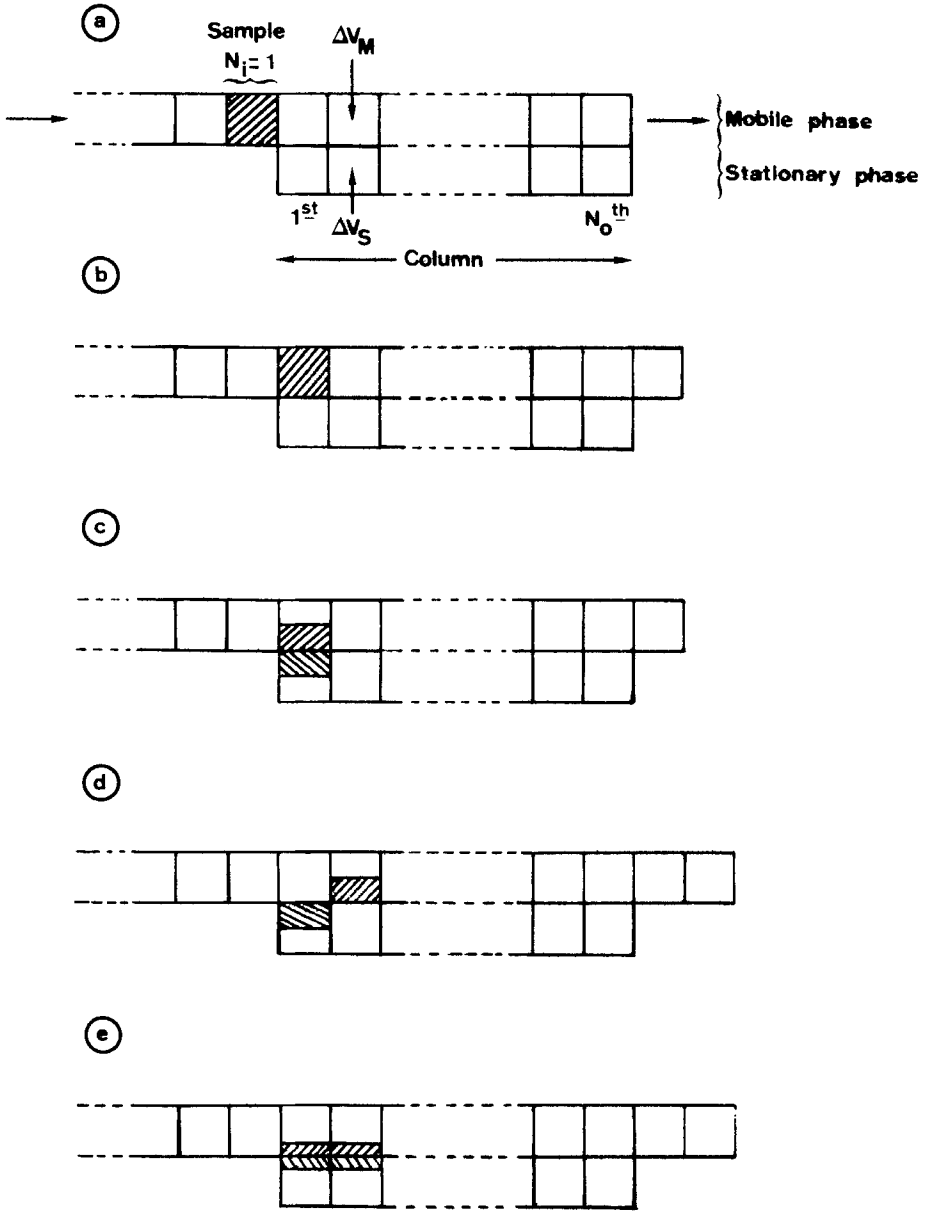

FIG. 4. Schematic diagram of a Craig machine.

mm i.d. with a total porosity ε equal to 0.8 and a dead volume equal to 2 mL; this column was divided into 100 stages.

Optimization of Injection Conditions

First, the chromatogram is simulated for various solute amounts Q_i injected in different injection volumes V_i. For each chromatogram the optimal fractionation volume V_c corresponding to a given recovery ratio r_0 of the solute of interest is determined and the corresponding purity p is calculated. From the p versus Q_i plots obtained for different V_i values (Fig. 5a), the variations of the reduced injectable load q_i corresponding to a given purity level p_0 against the reduced injection volume v_i are graphically determined (Fig. 5b).

Chromatographic Runs

Apparatus. The chromatograph consisted of a Model EC 93 solvent delivery system (Touzart & Matignon, Vitry/Seine, France) and a 10 cm × 2 cm i.d. longitudinally compressed column (Jobin Yvon, Longjumeau, France). For the injection of the samples, a Model 380 additional pump (Touzart & Matignon) was used.

Stationary Phases. The following commercially available stationary phases were used: Lichroprep Si-60, 5–20 μm (Merck, Darmstadt, FRG) and Lichroprep RP-18, 25–40 μm (Merck).

Solvents. All mobile phases were prepared from HPLC grade solvents (S.D.S., Peypin, France).

Samples. Bis(2-ethylhexyl)adipate, benzyl acetate, dimethyl phthalate and diethyl phthalate were of synthesis grade (Merck).

RESULTS

The different separation types considered in this study are classified according to the types of solute isotherms, and their parameters are given in Table 1. The type $M_A + M_B$ separation corresponds to the actual elution of dibutyl phthalate (Solute A) and diethyl phthalate (Solute B) on Lichroprep Si-60, 5–20 μm using the binary mixture 2,2,4-trimethyl-

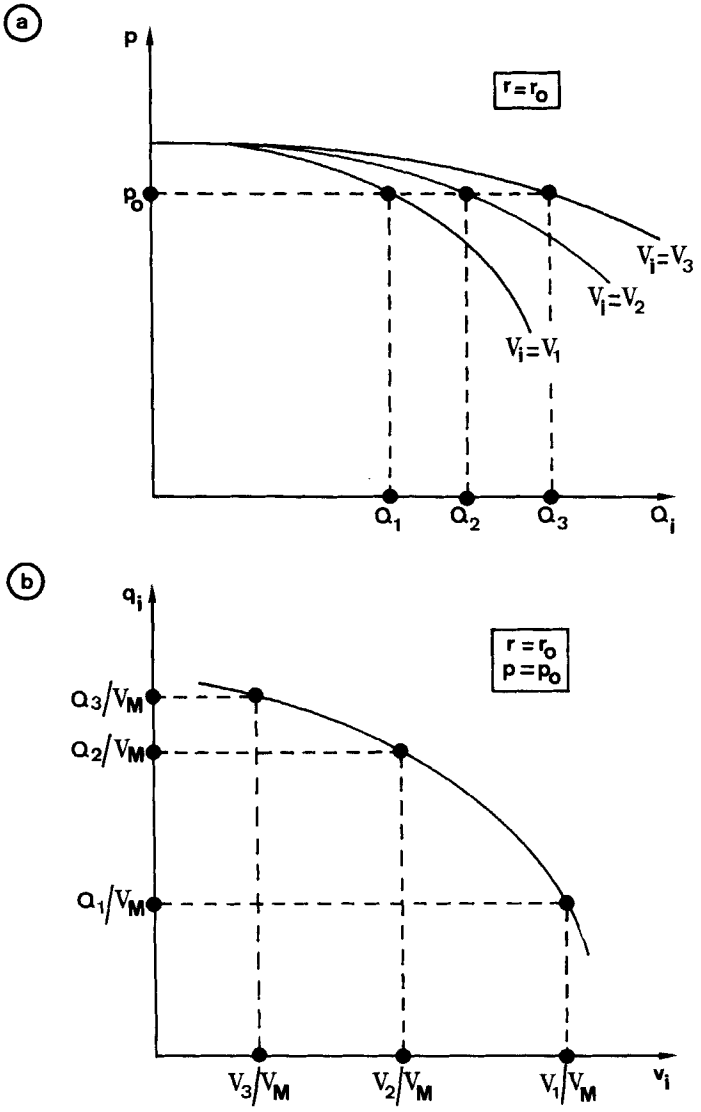

FIG. 5. Determination of the optimal injection conditions consistent with a given recovery ratio r_0 and a given purity p_0.

TABLE I
Classification of the Separation Types Considered

	Isotherm									
	Solute A					Solute B				
Separation type	Type	k'_A	a_A	b_A (L/mol)	$C_{B/A}$ (L/mol)	Type	k'_B	a_B	b_B (L/mol)	$C_{A/B}$ (L/mol)
$L_A + L_B$	L_A	1.3	5	+1	0	L_B	2.8	11.2	+1.4	0
$M_A + M_B$	M_A	1.3	5	+1	+0.2	M_B	2.8	11.2	+1.4	+0.05
$\bar{L}_A + \bar{L}_B$	$\bar{L}_A$	1.3	5	−1	0	$\bar{L}_B$	2.8	11.2	−1.4	0
$\bar{L}_A + L_B$	$\bar{L}_A$	1.3	5	−1	0	L_B	2.8	11.2	+1.4	0
$L_A + \bar{L}_B$	L_A	1.3	5	+1	0	$\bar{L}_B$	2.8	11.2	−1.4	0
$S_A + S_B$	S_A[a]	1.3	5	−1	0	S_B[b]	2.8	11.2	−1.4	0

[a] $C^0_{S,A} = 3$ mol/L.
[b] $C^0_{S,B} = 2$ mol/L.

pentane/ethyl acetate 90/10 v/v as eluent. The other separation types are considered theoretically. For each simulation the sample mixture is assumed to be equimolar except when some additional indication is mentioned.

Study of Column Overload from Calculated Elution Profile

Figures 6 to 10 illustrate the effect of mass overload on a chromatogram when the two solutes co-elute independently. Under mass overload conditions the peak shapes are strongly asymmetrical. Depending on the curvature of the distribution isotherm, either the elution volume of the peak front decreases while the elution volume of the peak rear remains almost constant, resulting in a sharp front and a tailing rear (convex type L_j isotherm), or the retention of the peak rear increases, resulting in a gradually ascending front and a sharply descending rear (concave type $\bar{L}_j$ isotherm). With a type S_j isotherm (that is, concave for low concentrations and convex for higher concentrations), the highly concentrated zones of the band migrate more slowly than the less concentrated ones (identically to a solute having a concave isotherm), but the peak front retention decreases while the peak rear retention is constant (identically to a solute having a convex isotherm).

As a result of column mass overload, the adjacent peaks broaden simultaneously and generally they end by overlapping. On the contrary, in the case of type $L_A + \bar{L}_B$ separation (an occasional but very advantageous case for preparative scale separation), as the injected sample load is increased, the peaks become more and more separated and never overlap.

Figure 11 shows the effect of volume overload for the type $L_A + L_B$ separation. The increase of the sample injection volume results in an essentially constant elution volume for the peak front while the peak rear is progressively shifted toward larger retention. This behavior under volume overload conditions does not depend on the solute isotherm shape. Therefore, for all the separation types, the peaks overlap when the column is volume overloaded. Figure 12 compares the situation in which each solute influences the distribution of the others (type $M_A + M_B$ separation), and the situation in which each solute elutes independently (type $L_A + L_B$ separation). Component A affects Component B by decreasing its retention volume. Similarly, Component B affects Component A by decreasing its retention volume but to a lesser extent. In the case of interactions between solutes, the earlier eluted peak is compressed while the later one is broadened. This phenomenon has been experi-

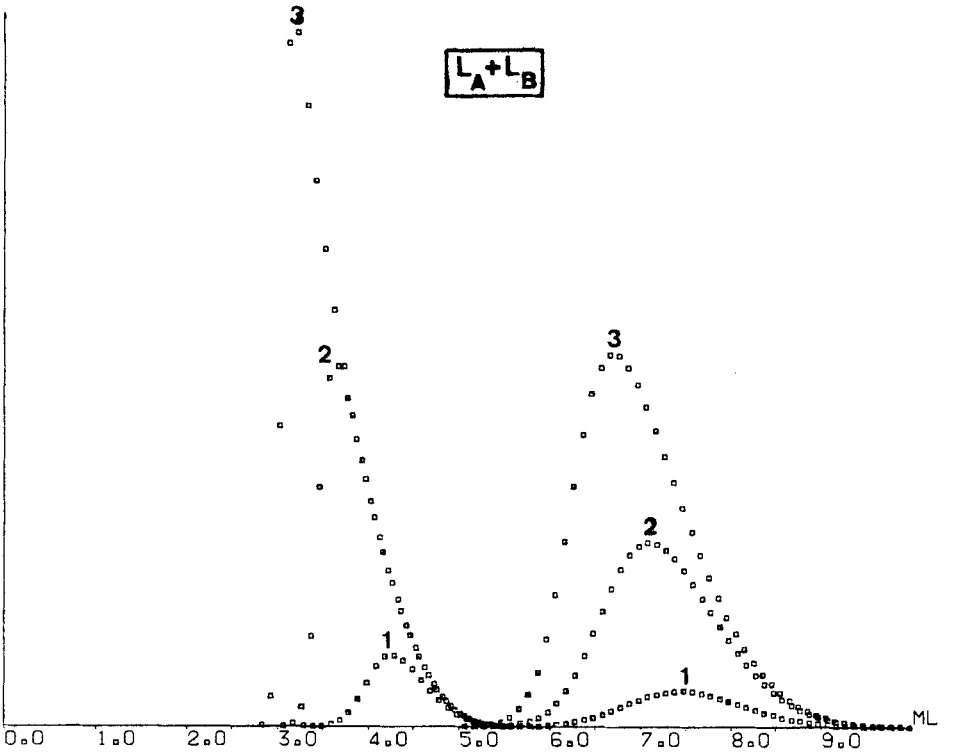

FIG. 6. Mass overload in the type $L_A + L_B$ separation. Injection volume $V_i = 0.02$ mL. Injected amount of each solute Q_i: (1) 4×10^{-5} mol, (2) 2×10^{-4} mol, (3) 4×10^{-4} mol.

mentally demonstrated by Gareil (*8*) and Eisenbeiss (*10*). Figure 13 describes situations in which the injected amount of Solute A is fixed while the injected amount of Solute B is varied. When the injected load of Solute B is decreased, A is less influenced by B and the elution profile of Solute A shifts to that obtained without any interaction between solutes (elution profile corresponding to the type L_A isotherm). This demonstrates the coherence of our chromatographic simulation algorithm.

Optimization of Injection Conditions from Simulated Chromatograms

Solute A is assumed to be the solute of interest. It is to be recovered with a 90% ratio and a 99.8% purity from an equimolar sample mixture.

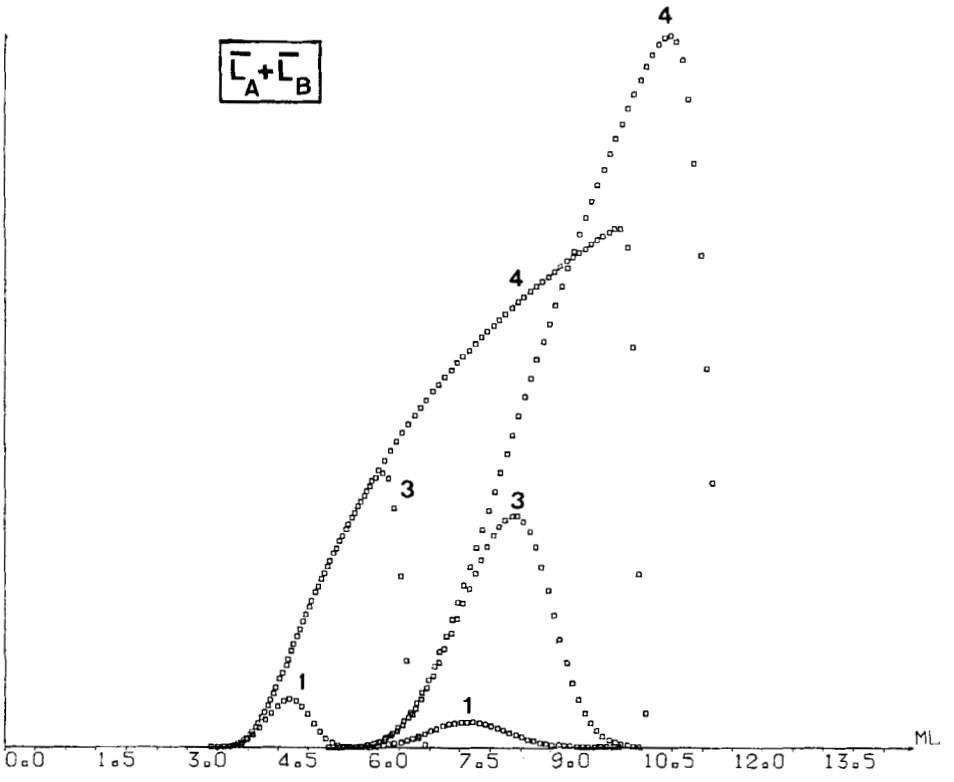

FIG. 7. Mass overload in the type $\bar{L}_A + \bar{L}_B$ separation. Same conditions as in Fig. 6. Injected Q_i: (4) 2×10^{-3} mol.

Figures 14 and 15 show the variations of the reduced injectable load q_i versus the reduced injection volume v_i for the different separation types. The case of type $L_A + \bar{L}_B$ separation is not presented because it is obvious from band broadening behavior that the injectable sample load is almost infinite provided the injection volume is kept minimum. For the other separation types, the shape of the q_i versus v_i plots is difficult to explain from band broadening behavior. Some plots (for separations of types $L_A + L_B$ and $S_A + S_B$) are continuously decreasing, which means that the smaller the injection volume, the larger the injectable sample load. For type $L_A + L_B$ separation, an identical result has been obtained using the Haarhoff-Van der Linde model (*2*). The other plots (for separation of types $M_A + M_B$ and $\bar{L}_A + \bar{L}_B$) exhibit a maximum, corresponding to an

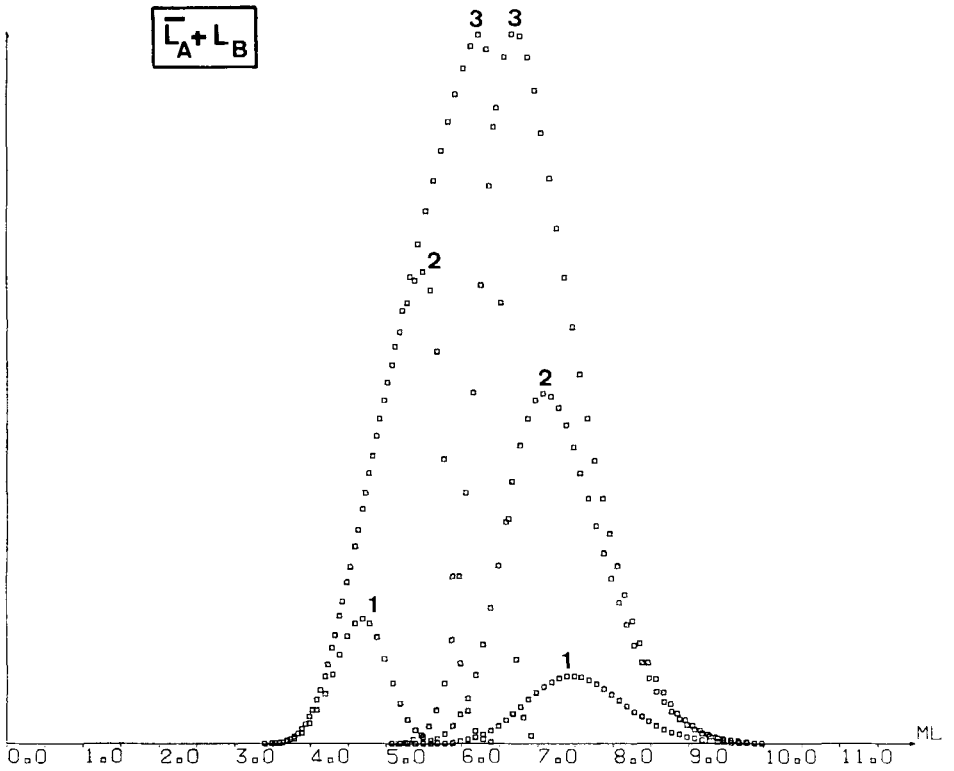

FIG. 8. Mass overload in the type $\bar{L}_A + L_B$ separation. Same conditions as in Fig. 6.

optimal injection volume. Under these isotherm conditions, excessive mass overload must be avoided. For type $\bar{L}_A + L_B$ separation, the existence of an optimal injection volume was obtained by peak simulation, using the Haarhoff-Van der Linde model (*14*). In conclusion, no general rule can be stated for optimizing injection conditions in preparative liquid chromatography. For samples poorly soluble in the mobile phase, determination of the optimal injection conditions is much more complicated. The injected concentration cannot be higher than the solubility limit S of the sample in the mobile phase. Figure 16 summarizes the different cases that can be found according to the shape of the q_i versus v_i plot. In all cases there is an optimal injection volume v_{op} (for which the injectable load is maximum) fixed either by the solubility limit of the sample in the mobile phase (Fig. 16b) or by the isotherm conditions (Fig. 16a, 16c, and 16d).

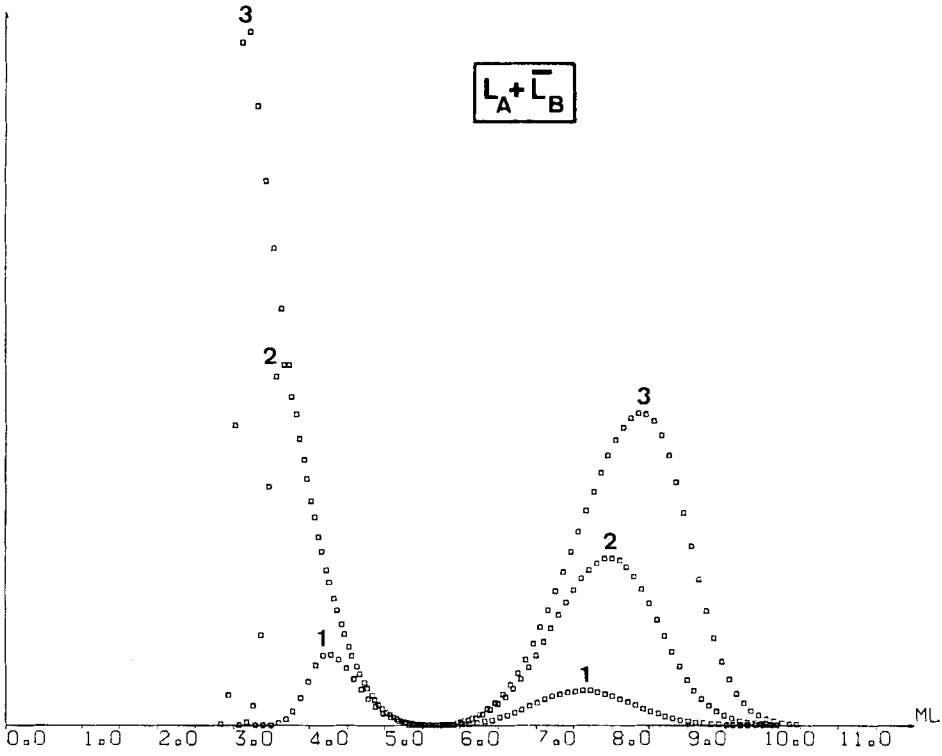

FIG. 9. Mass overload in the type $L_A + \bar{L}_B$ separation. Same conditions as in Fig. 6.

Optimization of Injection Conditions in Actual Separation Examples

In order to illustrate two of the different situations encountered in the optimization of injection conditions from simulated chromatograms, two actual separation examples were considered. Their experimental conditions and the corresponding separation types are mentioned in Table 2. Figures 17 and 18 show the chromatograms resulting from the injection of the same sample amount dissolved in different injection volumes for each separation example. In Example I (Fig. 17), the quality of the separation is decreased when the injection volume becomes larger than 1 mL; therefore, in this case, mass overload seems better than volume overload, which is in good agreement with the behavior simulated for a type $L_A + L_B$ separation. In Example II (Fig. 18), as simulated for a type

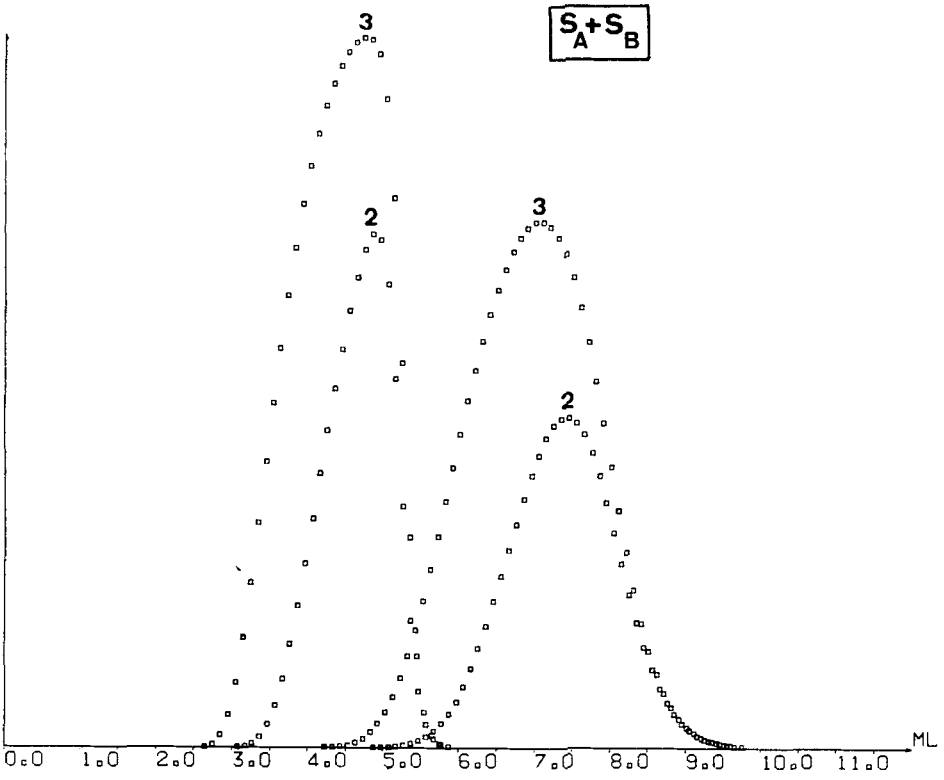

FIG. 10. Mass overload in the type $S_A + S_B$ separation. Same conditions as in Fig. 6.

$\bar{L}_A + L_B$ separation, there is an optimal injection volume equal to 1 mL under these conditions.

CONCLUSION

The foregoing discussion emphasizes that the optimization of the injection conditions consists of very complicated steps in the strategy for solving a preparative liquid chromatographic problem. The optimal injection conditions depend both on the isotherm and on the solubility limit of the sample in the mobile phase. In all cases there is an optimal injection volume V_{op} for which the injectable sample load is maximum.

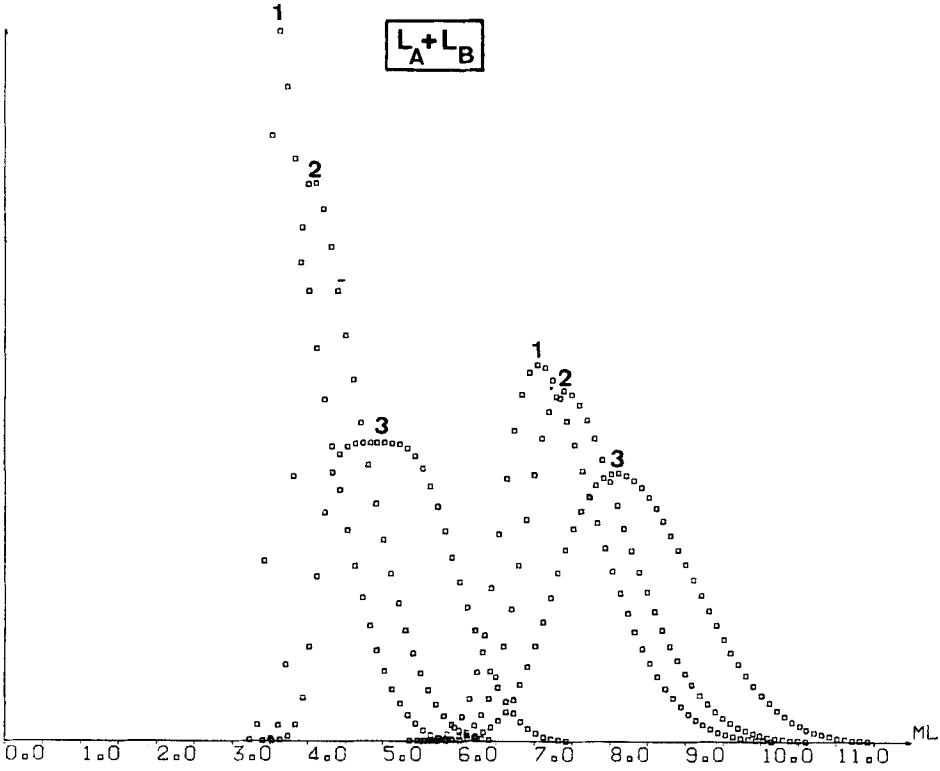

FIG. 11. Volume overload in the type $L_A + L_B$ separation. Injected amount of each solute Q_i: 4×10^{-4} mol. Injection volume V_i: (1) 0.5 mL, (2) 1 mL, (3) 2 mL.

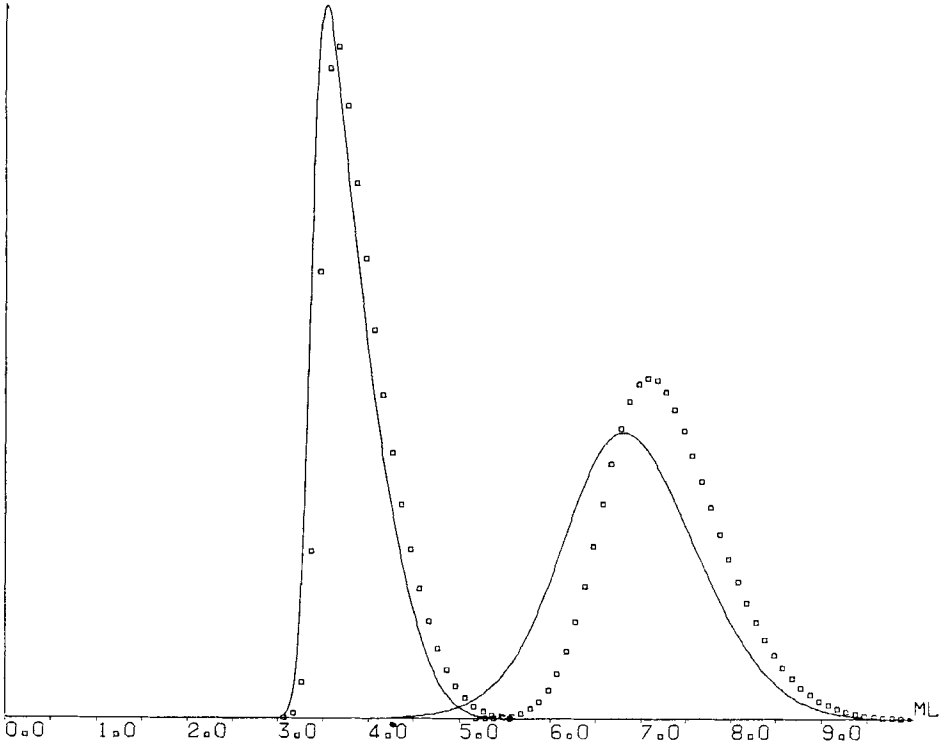

FIG. 12. Comparison between the type $M_A + M_B$ separation (——) and the type $L_A + L_B$ separation (□). Injection volume V_i: 0.02 mL. Injected amount of each solute Q_i: 2×10^{-4} mol.

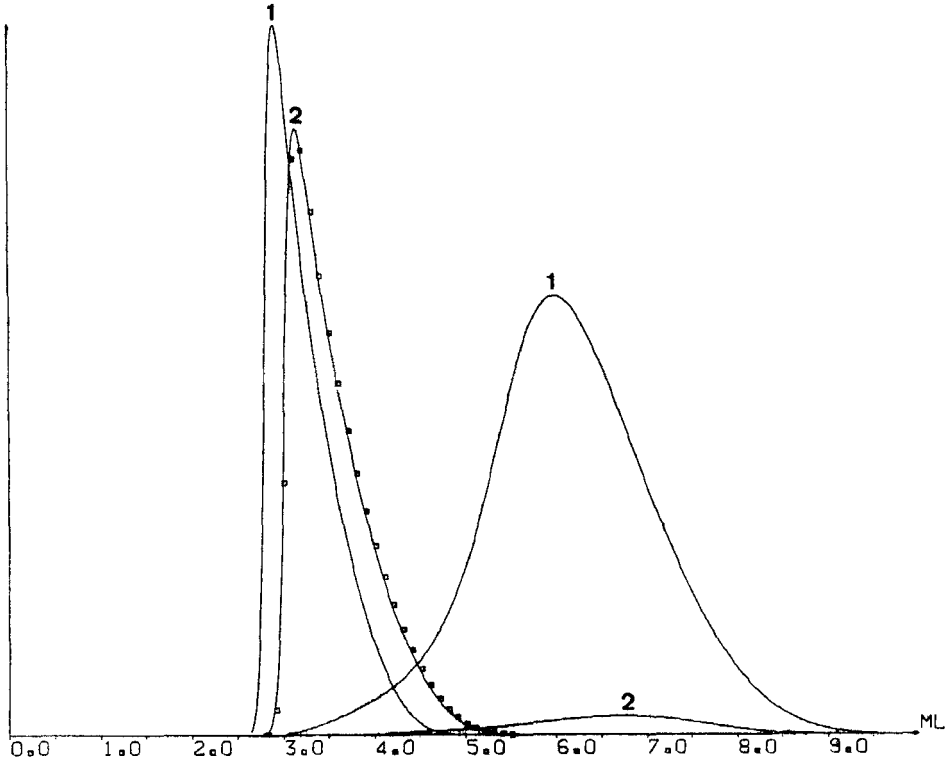

FIG. 13. Evolution of the chromatogram in the type $M_A + M_B$ separation (——) with the sample composition. Injection volume V_i: 0.02 mL. Injected amount of Solute A: 4×10^{-4} mol. Injected amount of Solute B: (1) 4×10^{-4} mol, (2) 4×10^{-5} mol. (□) Elution profile of Solute A corresponding to the injection of 4×10^{-4} mol in the type $L_A + L_B$ separation.

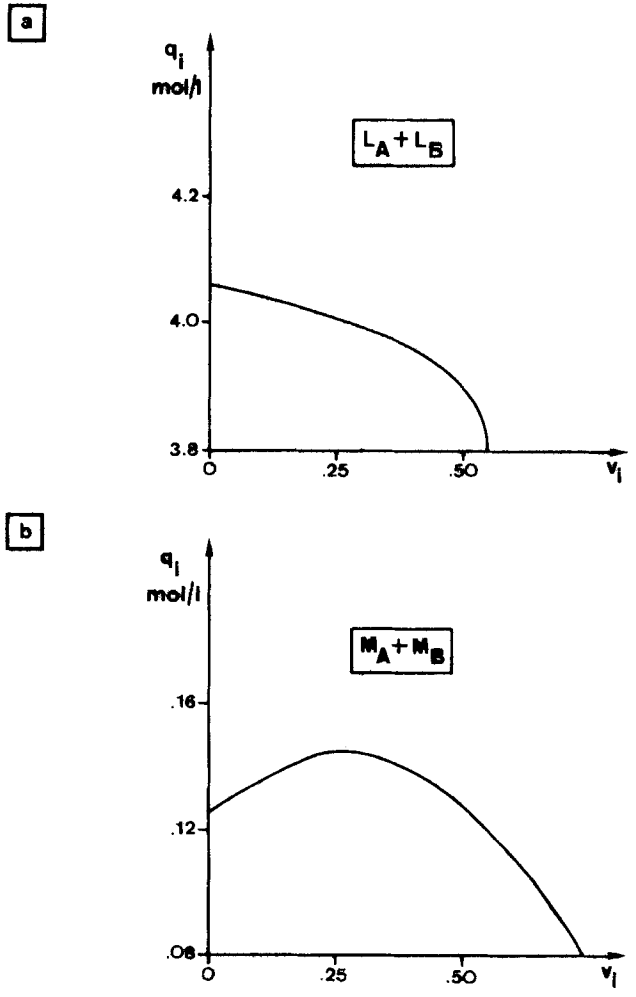

FIG. 14. Plots of the reduced injectable load q_i versus the reduced injection volume v_i for the separation types $L_A + L_B$ and $M_A + M_B$.

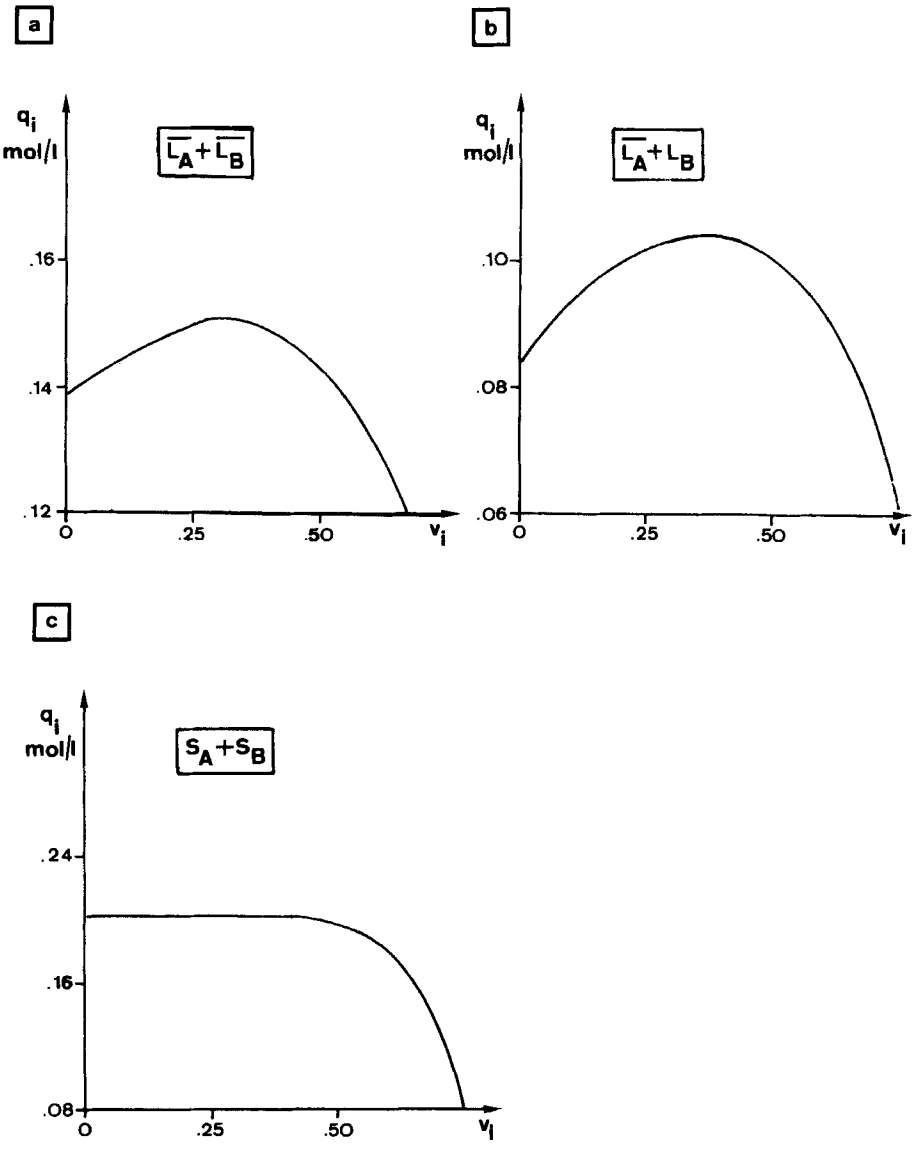

FIG. 15. Plots of the reduced injectable load q_i versus the reduced injection volume v_i for the separation types $\bar{L}_A + \bar{L}_B$, $\bar{L}_A + L_B$, and $S_A + S_B$.

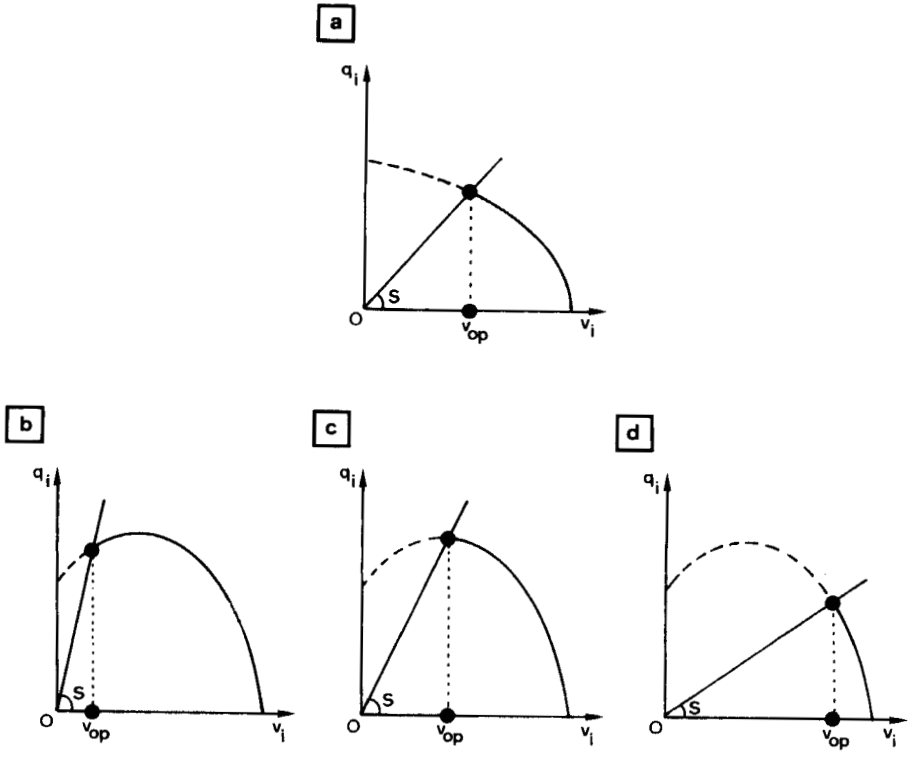

FIG. 16. Influence of the solubility limit S of the sample in the mobile phase on the optimization of the injection conditions.

TABLE 2
Experimental Conditions of the Separation Examples

Example	Solute A	Solute B	Sample Composition Solute A/ Solute B (w/w)	Stationary phase	Mobile phase	Separation type
I	Dimethyl phthalate	Diethyl phthalate	2/1	Lichroprep RP-18, 25–40 μm	Methanol/water, 70/30 v/v	$L_A + L_B$
II	Bis(2-ethylhexyl) adipate	Benzyl acetate	1/1	Lichroprep Si-60, 5–20 μm	*n*-Heptane/ethyl acetate, 95/5 v/v	$\bar{L}_A + L_B$

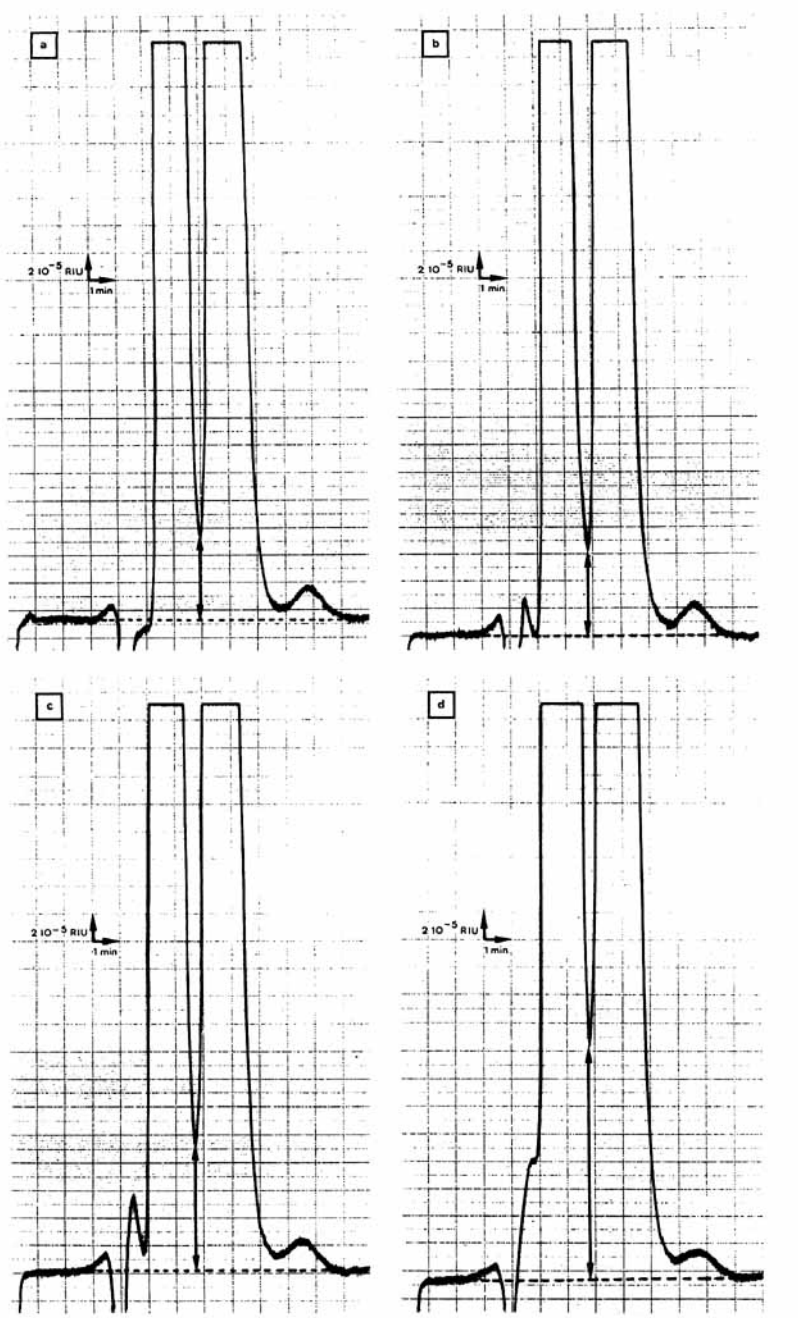

FIG. 17. Example I. Injected amount of Solute A: 100 mg. Injected amount of Solute B: 50 mg. Injection volume: (a) 0.5 mL, (b) 1 mL, (c) 2 mL, (d) 4 mL.

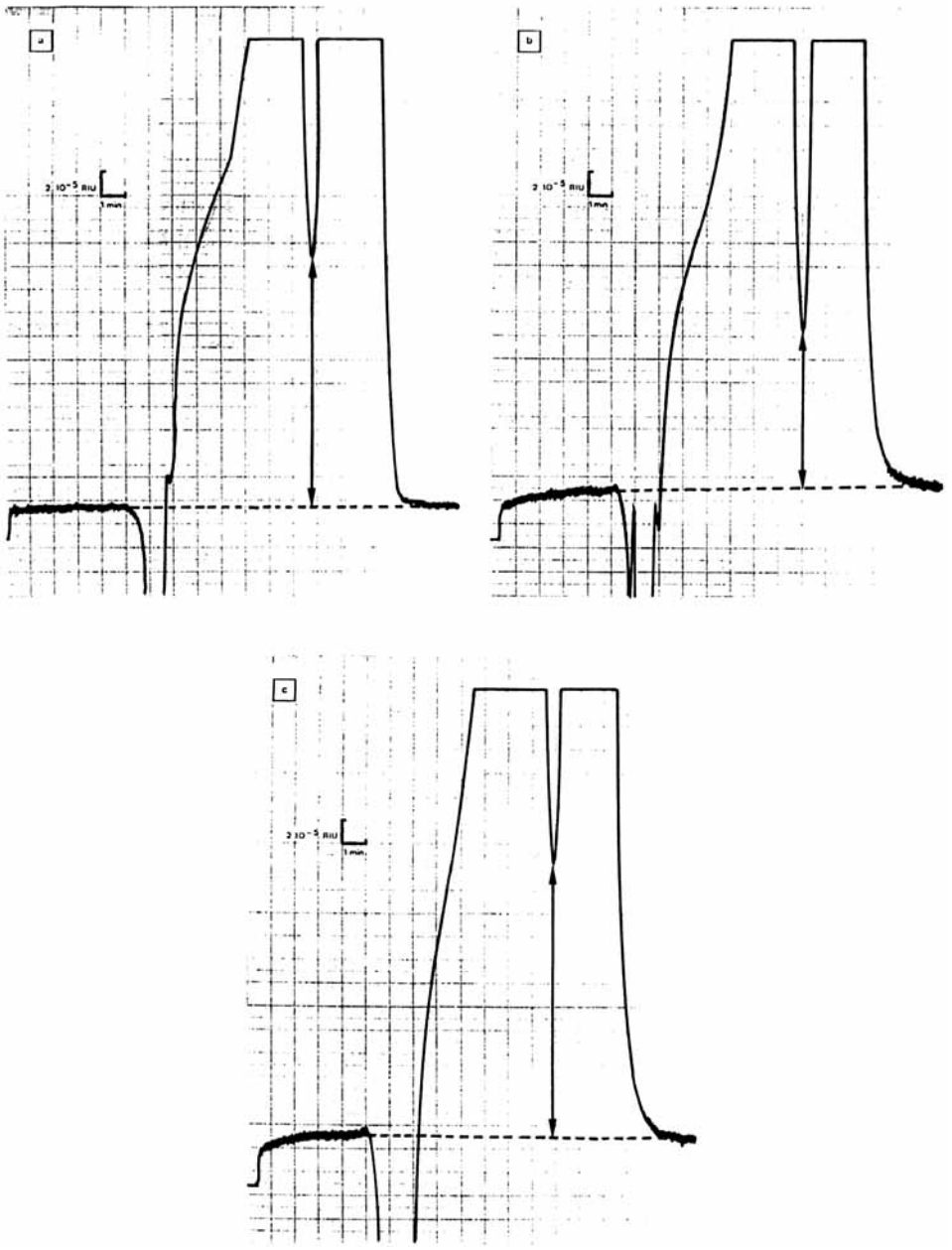

FIG. 18. Example II. Injected amount of each solute: 200 mg. Injection volume: (a) 0.5 mL, (b) 1 mL, (c) 2 mL.

For a sample very poorly soluble in the mobile phase, large injection volumes are required more often, and V_{op} is determined only by the solubility limit of the sample in the mobile phase. For a sample more soluble in the mobile phase, V_{op} is determined either by the solubility limit or by the solute isotherm characteristics and the separation type. Unfortunately, for the experimental determination of the optimal injection conditions, no general rule can be stated. The trial-and-error method is necessary even though it is often a time-consuming step.

REFERENCES

1. P. Gareil, C. Durieux, and R. Rosset, *Sep. Sci. Technol., 18,* 441 (1983).
2. G. Cretier and J. L. Rocca, *Chromatographia, 20,* 461 (1985).
3. L. S. Brunauer, W. E. Deming, and E. Teller, *J. Am. Chem. Soc., 62,* 1723 (1940).
4. C. H. Giles, T. H. MacEwan, S. N. Nakhwa, and D. Smith, *J. Chem. Soc.,* p. 3973 (1960).
5. R. S. Henly, A. Rose, and R. F. Sweeny, *Anal. Chem., 36,* 744 (1964).
6. F. Helfferich and G. Klein, *Multicomponent Chromatography—Theory of Interference,* Dekker, New York, 1970.
7. R. P. W. Scott and P. Kucera, *J. Chromatogr., 119,* 467 (1976).
8. P. Gareil, Thesis, Paris, 1981.
9. S. Seshadri and S. N. Deming, *Anal. Chem., 56,* 1567 (1984).
10. H. Eisenbeiss, A. Wehrli, and J. F. K. Huber, *Chromatographia, 20,* 657 (1985).
11. C. N. Reilley, G. P. Hildebrand, and J. W. Ashley, *Anal. Chem., 34,* 1198 (1962).
12. B. L. Karger, L. R. Snyder, and C. Horvath, *An Introduction to Separation Science,* Wiley, New York, 1973, p. 116.
13. A. Gourdin and M. Boumarhat, *Méthodes numériques appliquées,* Lavoisier, Paris, 1983.
14. G. Cretier, C. Ponthus, and J. L. Rocca, Unpublished Results, University of Lyon, 1986.